OPTIMISATION OF PROCESS PARAMETERS OF INDUCTION-BASED FRICTION STIR WELDING OF CAST NYLON

B. Akhila Bai¹, P. Prasanna²

¹Post Graduate Student, Department of Mechanical Engineering, Jawaharlal Nehru Technological University, Hyderabad, Telangana,

²Associate Professor, Department of Mechanical Engineering, Jawaharlal Nehru Technological University, Hyderabad, Telangana

ABSTRACT: Friction Stir Welding (FSW) is a solid-state method that avoids melting and offers promise for thermoplastics, which are difficult to join by fusion. This study examines induction-assisted FSW (i-FSW) for Cast Nylon-6A, chosen for its wear resistance and dimensional stability. To address uneven heat in conventional FSW, an external induction system was coupled with a high-speed steel pin tool, providing localized preheating to improve plastic flow and weld strength.

Numerical simulations in ANSYS Workbench modelled thermal—mechanical behaviour across tool speeds, traverse speeds, and axial loads, targeting a 140–180 °C softening window. Higher rotational speeds and axial loads enhanced heating uniformity, penetration, and conduction. The best results appeared at 1200 RPM, 15 mm/min, and 150 Kgf, with tool-tip temperatures close to shoulder levels.

Experiments used tensile, hardness, and Izod tests on 27 parameter sets arranged by a Taguchi L27 design. Results confirmed the simulations: the optimum set (1200 RPM, 15 mm/min, 150 Kgf) achieved 60.87 MPa tensile strength with high hardness and toughness. ANOVA and regression validated these outcomes.

Induction acted as in-situ annealing, improving weld quality and efficiency. Compared to non-induction FSW, induction doubled production without loss of strength. At 25 mm/min, it outperformed the best non-induction welds, and at 30 mm/min, it retained competitive strength while raising throughput. Overall, i-FSW proved effective for thermoplastics by enhancing heat control, mechanical performance, and productivity.

1. INTRODUCTION

1.1 Introduction

Welding remains a cornerstone process in industrial manufacturing, widely applied across sectors for assembling components and structures. However, welding certain materials—particularly aluminium and its alloys—presents ongoing challenges due to their high thermal conductivity and relatively low melting point. These properties complicate the use of conventional fusion welding methods, often resulting in defects or weak joints. In marine environments, the difficulty intensifies; welding tasks on structures such as ships, underwater pipelines, and offshore platforms necessitate operations in submerged conditions, where traditional arc welding methods pose significant safety and operational hazards. To overcome such limitations, a solid-state joining process known as Friction Stir Welding (FSW) has emerged. This innovative technique offers a safer and more effective alternative for joining metals and polymers alike, particularly in complex or high-risk environments.

Friction Stir Welding (FSW), introduced in 1991 by Wayne Thomas at The Welding Institute (TWI) in the UK, is a solid-state joining process that has gained widespread recognition for its ability to weld materials that are traditionally challenging to join, such as aluminium alloys. Operating below the melting point of the base materials, FSW avoids many of the defects commonly associated with conventional fusion welding techniques, such as porosity, cracking, and distortion. Since its development, the process has become the subject of extensive research and industrial application due to its superior mechanical properties and reliability [1].

FSW relies on mechanical friction rather than an external heat source or filler material, making it a cleaner and more energy-efficient alternative. The process creates strong, high-quality joints while preserving the material's microstructure and minimising thermal degradation. Its ability to maintain the integrity of the base materials while producing consistent, defect-free welds has made it highly suitable for critical applications in industries such as aerospace, automotive, marine, and rail transportation [2].

1.2 Working Principle of Friction Stir Welding (FSW)

The process involves a specially designed, non-consumable rotating tool composed of a pin and a shoulder. This tool is inserted into the joint line between two rigidly clamped workpieces. As the tool rotates and travels along the joint, friction between the tool and the material generates localised heat. This heat softens the material without reaching its melting point. The softened material is then stirred and forged by the motion of the tool, allowing the two pieces to bond at a molecular level under axial pressure.

As the tool advances, plasticised material is swept from the front of the pin to the rear, where it cools and solidifies, forming a high-strength weld. The shoulder helps contain the softened material and applies the necessary forging force to consolidate the joint. This combination of mechanical stirring and pressure ensures a uniform, defect-free weld. Additionally, the process minimises issues commonly associated with fusion welding—such as porosity, solidification cracking, and spatter—making FSW a clean, efficient, and reliable method for both industrial and structural applications [1]

1.3 Process Parameters in Friction Stir Welding

Friction Stir Welding (FSW) is a complex thermo-mechanical process influenced by a variety of interconnected parameters. These parameters determine the material flow, heat input, and ultimately the mechanical and microstructural quality of the weld. The key process parameters are detailed and listed below:

- **Tool Rotation Speed:** Controls frictional heat. Low speed causes weak bonding; high speed may over-soften the material, creating defects.
- **Tool Traverse Speed:** Affects heat exposure time. High speed may result in poor mixing; low speed can cause overheating and soft weld zones.
- **Axial Force:** Ensures tool penetration and bonding. Too low causes shallow welds; too high may deform the workpiece.
- **Tilt Angle:** Helps in forging action. Optimal tilt enhances weld quality, but extreme angles may result in voids or incomplete welds.
- **Shoulder Diameter:** A Larger diameter increases heat and material retention. It must be balanced to avoid overheating or spillage.
- **Pin Profile:** Shapes like cylindrical, threaded, or tapered influence material flow and mixing. Proper selection minimises weld defects.

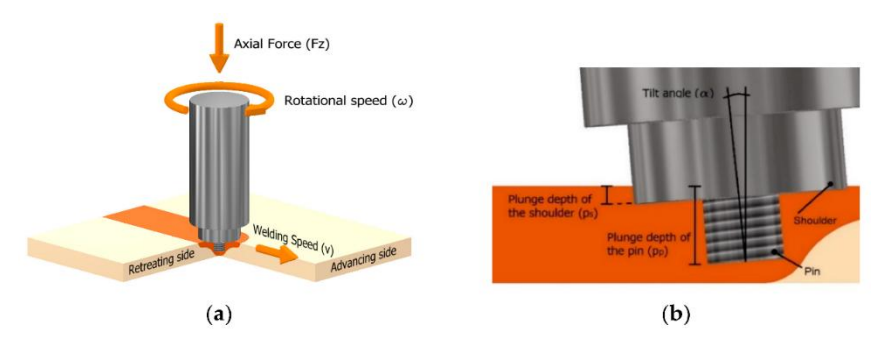


Figure 1.1: (a) Friction Stir Welding Process (b) Weld Cross-Sectional View [1]

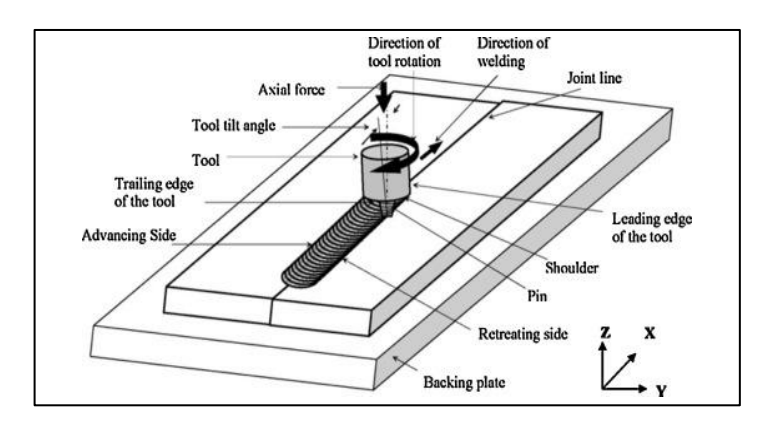


Figure 1.2: Schematic Diagram of Friction Stir Welding Process [3]

1.4 Welding Metallurgy

The welding metallurgy of Friction Stir Welding (FSW) involves significant changes in the material's microstructure resulting from localised heat generation and mechanical stirring. The welded joint is typically divided in four distinct zones based on the degree of thermal and mechanical influence. At the core lies the Stir Zone (SZ), also known as the Nugget Zone, where the rotating pin causes intense plastic deformation and dynamic recrystallisation, resulting in fine, equiaxed grains and a distinct "onion ring" pattern indicating proper material flow. Surrounding the stir zone is the Thermo-Mechanically Affected Zone (TMAZ), which experiences both heat and some degree of deformation, but not enough to fully recrystallise the grains; instead, the grains appear elongated and distorted. Adjacent to the TMAZ is the Heat-Affected Zone (HAZ), where the material is exposed to the welding temperature without mechanical disruption. In this region, thermal effects may alter the properties of heat-sensitive materials, sometimes reducing their strength. Finally, beyond the HAZ lies the base material, or parent zone, which remains unaffected by the welding process.



Figure 1.3: Schematic Representation of the Cross-Sectional HAZ in a FSW [4]

2. Methodology

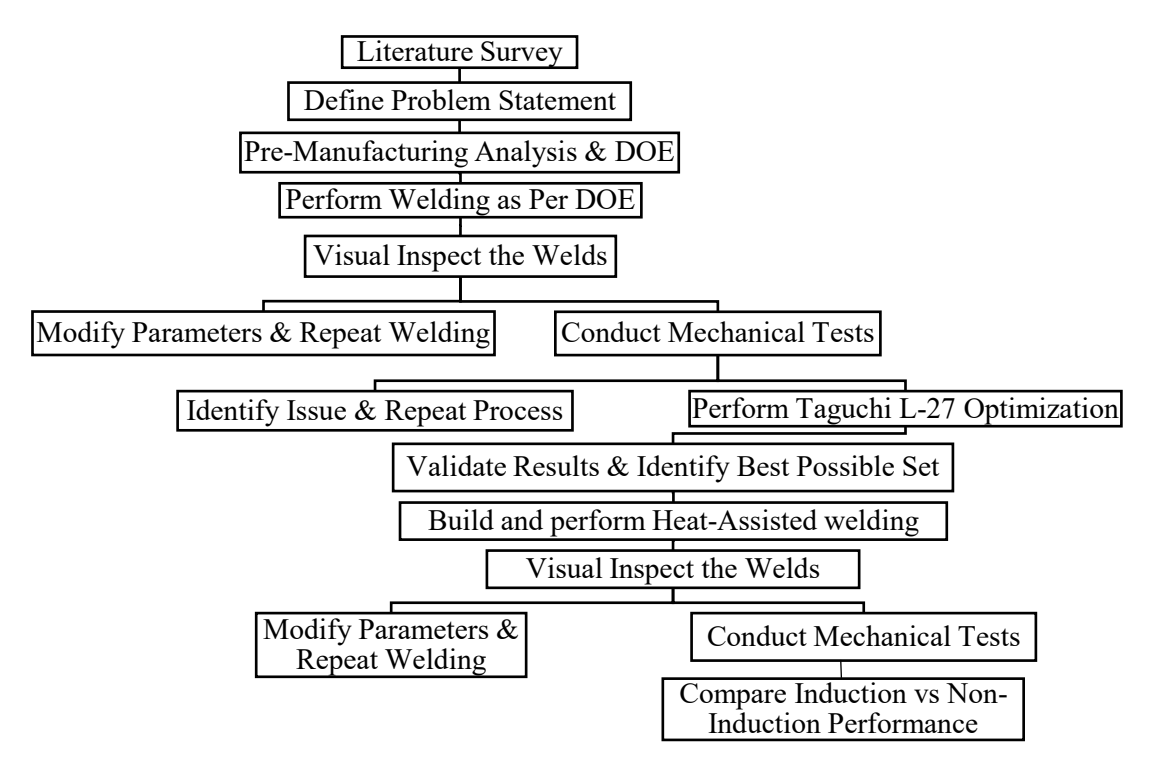


Figure 2.1: Methodology

2.1 Material selection

2.1.1 Material Used – Cast Nylon

In this study, Cast Nylon was selected as the base material for Friction Stir Welding (FSW) due to its superior mechanical strength, excellent wear resistance, and dimensional stability. Cast Nylon is a type of polyamide that is produced by the controlled polymerisation of caprolactam monomer directly into moulds. This casting process yields a high degree of crystallinity, resulting in nylon components with enhanced properties compared to those produced by extrusion or injection moulding. These features make Cast Nylon ready for industrial applications such as gears, bushings, rollers, sheaves, wear pads, and automotive components.

The suitability of Cast Nylon for friction stir welding was assessed based on its thermal properties, mechanical robustness, and ability to withstand localised heating during the welding process. Its behaviour under thermal-mechanical loads made it a strong candidate for use in the present study, particularly when combined with induction-assisted heating to improve weld quality. [5]

2.1.2 Properties of Cast Nylon

- Coefficient of Thermal Expansion (CTE): The CTE describes how much a material will change in size as the temperature changes. Materials with a higher CTE expand more when heated and contract more when cooled.
- Young's Modulus: Stiffer materials resist deformation and can limit material flow.

- **Poisson's Ratio:** Poisson's ratio shows how much a material expands sideways under load. In FSW, a moderate value is preferred to balance flow and residual stresses.
- Coefficient of friction: Drives heat generation.
- Conductivity: High conductivity spreads heat evenly, reducing hot spots and residual stress. Low values risk localised overheating. However, very high conductivity can dissipate heat too quickly, leading to cold spots and brittle welds.
- Glass Transition Temperature (Tg): Tg (~60°C for cast nylon) is the temperature at which the material transitions from a hard, glassy state to a soft, rubbery state. SFW must exceed Tg to enable plastic deformation. Welding below Tg leads to brittle behaviour and weak joints.
- Solvus (Solidus) Region (Welding Region): In cast nylon, the solidus region begins immediately after the glass transition temperature (approximately 60°C) and extends up to its melting point (around 190°C).

•	I [-1)[-1
Material Properties	Values
Mechanical and Ph	nysical Properties
Density	1.17 g/cm^3
Youngs Modulus	2x10 ⁵ MPa
Poisson's Ratio	0.30
Yield Strength	55 MPa
Compressive Yield Strength	61.1 MPa
Ultimate Tensile Strength	75.8 MPa
Coefficient Of Friction	0.24
Elongation % @ Break	20 %
Impact Strength (Izod)	0.6 J/cm
Hardness Scale M	82-88
K Wear Factor	219*10 ⁻⁸ mm ³ /Nm
Thermal P	roperties
Coefficient Of Thermal Expansion	8.6x10 ⁻⁵ 1/°C
Isotropic Thermal Conductivity	0.271 W/m °C
Glass Transition Temp	60 °C
Melting Point	190 °C
Maximum Service Temp	180 °C
Specific Heat Capacity	1.55 J/g

Table 2.1: Cast Nylon Mechanical & Thermal Properties [6], [7]

2.2 Applications of Cast Nylon for Friction Welding

When Cast Nylon sheets are joined using Friction Stir Welding (FSW)—especially with Induction-based Friction Stir Welding (IFSW)—the resulting welds retain much of the material's original properties and allow the fabricated parts to be used in various engineering and industrial applications where high strength, wear resistance, and dimensional stability are critical. [5]

2.3 Experimental setup of the FSW machine

The CNC-based Friction Stir Welding (FSW) machine features a vertical spindle equipped with a collet-mounted FSW tool. The workpiece is securely fixed on the machine's bed using a rigid fixture, and clamps are applied to hold the specimens firmly in place,

preventing any lateral or transverse movement during welding. Once the specimens are correctly positioned and the welding parameters are programmed into the CNC controller, the rotating FSW tool is gradually lowered until its tool shoulder makes contact with the specimen's surface, ensuring precise engagement between the tool and material.



Figure 2.2: CNC-Controlled Friction Stir Welding (FSW) Machine (JNTU-H)

2.4 Tool Design:

In friction stir welding (FSW), tool geometry affects material flow and determines the optimal traverse rate. The tool pin, slightly shorter than the workpiece thickness, penetrates the joint line while the shoulder remains in contact with the surface. This design facilitates three critical functions: localised heating through friction, stirring of the softened material, and forging of the weld seam. Initially, most heat is generated by friction between the pin and the workpiece. At the same time, the shoulder contributes substantially once in full contact, helping to contain and regulate the heated volume. Tool geometry—especially the ratio between the shoulder and pin—plays a crucial in microstructural homogeneity and stress distribution. In this project, a cylindrical pin tool made of High-Speed Steel (HSS) is employed. This type of tool was selected due to its simplicity, ease of fabrication, and effective performance in generating adequate heat & material flow during the FSW process.

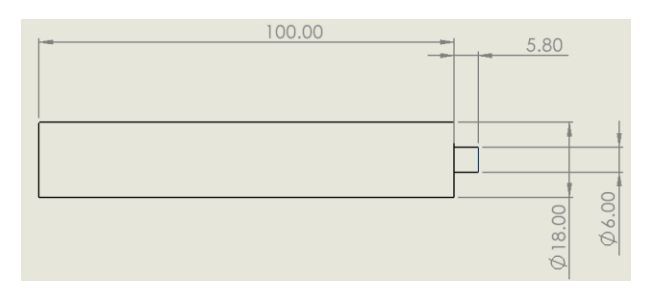


Figure 2.3: Dimensions of Cylindrical Pin Profile Tool CAD Drawing



Figure 2.4: FSW Cylindrical Pin Profile Tool - HSS



Figure 2.5: Friction Stir Welded Cast Nylon Plate

2.5 Induction Assisted Friction Stir Welding Setup

The induction coil is connected to the power supply unit via wires, generating the required electromagnetic field for heating. A temperature sensor placed near the tool continuously monitors its temperature and sends feedback to the temperature control system. The power supply adjusts the output based on this feedback to maintain the desired temperature. This integrated setup ensures precise and controlled induction heating of the FSW tool during the welding process. In this project, improving the production rate is a key priority. The integration of induction heating directly supports this goal by enabling faster weld speeds and minimising the downtime caused by tool wear or inconsistent welds. This ensures high-quality output without compromising efficiency. Induction heating helps reduce tool wear, enhance material flow, increase production rates, and improve joint strength, especially for thermoplastics and high-melting-point metals. [3]

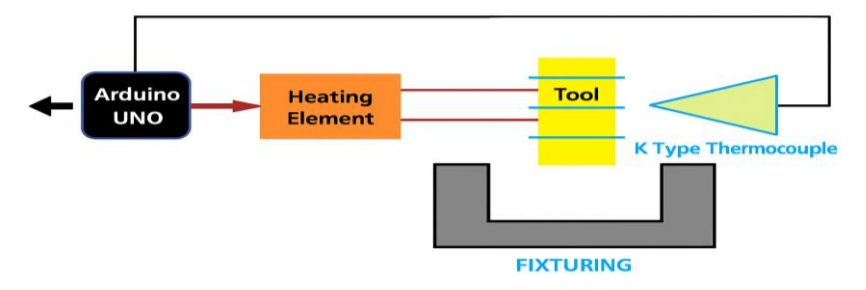


Figure 2.6: Induction Assisted Friction Stir Welding Setup Working Schematic

2.5.1 Induction Setup Design and Building

In this induction heating setup, an input AC power source feeds the power supply unit, which converts it to a controlled DC output suitable for induction heating. The DC output is delivered through wires to the induction coil, which is wrapped around or positioned near the tool. The coil generates a high-frequency alternating magnetic field, inducing eddy currents in the tool, thereby heating it. A sensor attached near the tool monitors its temperature. It sends signals to the temperature control system, which adjusts the power supply output to maintain the desired temperature. This closed-loop system ensures precise heating for induction-assisted SFW.

Induction heating is integrated into the friction stir welding (FSW) process to enhance weld efficiency and quality, particularly when production rate is a primary objective. When working with thermoplastics like cast nylon or other difficult-to-weld materials, the

induction setup provides controlled, localised heating to the weld zone without direct contact. This preheating softens the material before and during stirring, reducing the forces required for welding and improving material flow.

In this project, induction heating enables cast nylon to reach its solidus region more quickly and uniformly, promoting a softened state without melting. This setup was mounted on an outsourced CNC Milling Machine in kushaiguda, Hyderabad, Telangana.

Table 2.2: Components used to Develop Induction System [9], [10], [11], [12], [13]

S.No	Component	Description / Function	Pictorial Representation	Qty.
1	12V Rechargeable Battery/Converter	Powers the heating element and electronics (portable source)		1
2	Arduino Uno	Microcontroller to control temperature, relay, display, etc.	USC OF THE PROPERTY OF THE PRO	1
3	Temperature Sensor (e.g., LM35, DS18B20)	Measures the temperature at the weld zone		1
4	Relay Module (1- Channel or 2- Channel)	Switches the heating element ON/OFF based on sensor readings		1
5	12V DC Jack (Male + Female)	Connects battery to system (safe and detachable power interface)		1 set
6	Heating Element (12V, ceramic or coil type)	Provides controlled heat to assist plastic flow		1
7	LCD Display 16x2 (with I2C module if possible)	Displays temperature and system status		1



Figure 2.7: Induction System Setup on FSW Machine

2.6 Tensile test:

The tensile and notch tensile strengths of the friction-stir-welded cast nylon plates were evaluated following the EN 12814-2:2021 standard for testing welded joints of thermoplastic. This standard outlines procedures for specimen preparation, test dimensions, and testing conditions to determine the tensile strength of the weld created. Tensile tests were carried out on a universal testing machine (UTM) in the Mechanical Testing Laboratory at JNTU Hyderabad.

2.6.1 Tensile Test Specimen

Flat plate specimens were preferred over dog-bone specimens for weld tensile testing because they offer a larger, uniform cross-section that fully includes the weld region. This ensures that failure occurs in the weld if it is weaker or equal in strength to the base material, providing a more accurate assessment of weld strength. In contrast, dog-bone specimens have a reduced gauge section that often excludes much of the weld, frequently causing failure in the weld area due to stress concentration. While dog bone specimens can still accurately evaluate weld strength, they are more tedious to fabricate with precise dimensions. Furthermore, using flat plates allows testing a larger portion of the weld, enabling a broader inspection area for potential defects—similar to how 4-point bending tests offer a broader evaluation scope than 3-point bending tests—leading to more accurate and comprehensive results.

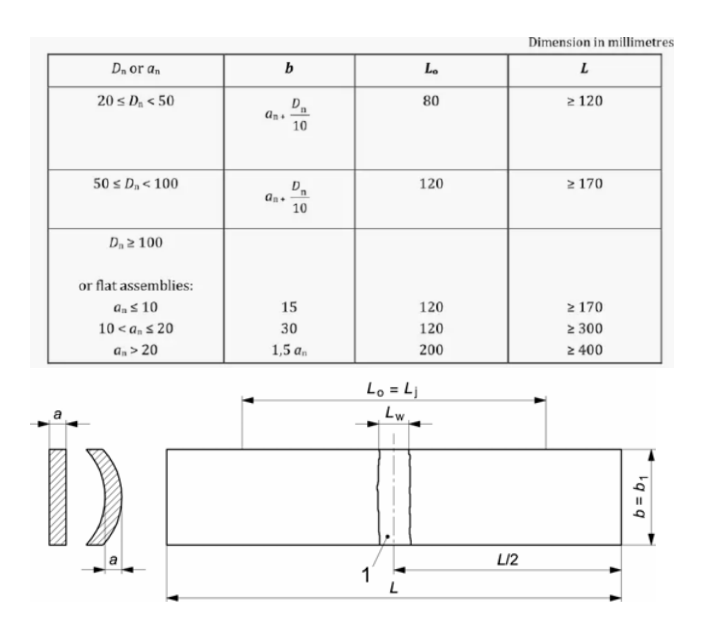


Figure 2.8: Tensile Test Standard Specimen SIST EN 12814-2:20 with Dimensions [14]

Here: an = specimen width for flat assemblies
Dn = nominal outer diameter for tubes
b = specimen width

Lo = gauge length L = total specimen length

2.7 Rockwell hardness test

The Rockwell hardness test is a quick method to measure resistance to indentation using a steel or carbide indenter under load, with penetration depth giving a direct hardness value. Different Rockwell scales (A, B, C, D, M) are used depending on material type.

For the welded cast nylon joints, the Rockwell M-scale was chosen as per standards for thermoplastics like nylon and polystyrene. A 1/4-inch steel ball indenter with a 100 kg load was used, and readings were taken on the red dial. This test provided localized hardness near the weld zone, reflecting the thermal and mechanical effects of welding.



Figure 2.9: Rockwell-M Hardness Test Specimens

2.8 Izod Impact Test

The Izod impact test measures a material's toughness under sudden loading by recording the energy absorbed when a notched specimen is struck by a pendulum. The absorbed energy, expressed in joules per centimetre (J/cm), reflects the material's resistance to fracture. In this test, the specimen is clamped vertically with the notch facing the pendulum, and the energy lost during fracture corresponds to the impact strength. This standardized method provides a consistent way to compare the toughness of metals, plastics, and composites, making it useful in quality control and material selection.

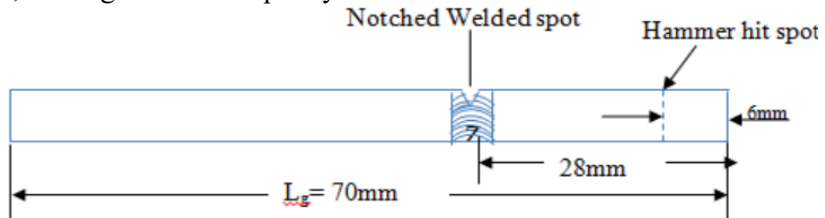


Figure 2.10: Modified ASTM D-256 Izod Test Specimen [16]



Figure 2.11: Izod Impact Fractured Specimen

2.9 Taguchi Optimisation (L27)

In this study, the Taguchi L27 orthogonal array was employed to optimise the process parameters of friction stir welding—tool rotational speed, welding speed, and axial load—at three levels each. The L27 design was selected instead of a smaller L9 array, as it not only reduces the number of experimental trials but also enables the analysis of both main effects & parameter interactions, which play a significant role in welding performance. [17]

1. Signal-to-Noise (S/N) Ratio Analysis

To evaluate the effect of each parameter on mechanical properties, the signal-to-noise (S/N) ratio approach was applied using Minitab software. This method balances mean performance with variability, thereby identifying the optimal parameter settings [18]. Depending on the nature of the response, different S/N formulations were used:

• Larger is Better: applied to maximise responses such as Yield Strength, UTS, Hardness, and Toughness.

$$S/N = -10 \cdot \log_{10} \left(rac{1}{n} \sum rac{1}{Y^2}
ight)$$

• Nominal is Best: used when the target value is fixed.

$$S/N = 10 \cdot \log_{10} \left(rac{ar{Y}^2}{s^2}
ight)$$

• Smaller is Better: used to minimise undesirable responses.

$$S/N = -10 \cdot \log_{10} \left(rac{1}{n} \sum Y^2
ight)$$

Where:

Y = observed response

 s^2 = variance.

n = number of replications

 \bar{Y} = mean response

2. Analysis of Variance (ANOVA)

Following S/N analysis, ANOVA is performed to determine statistical significance & percentage contribution of the factors. ANOVA partitions the total variability of the data into between-group variability (due to process parameters) and within-group variability (error/noise). The F-ratio and P-value were used as decision criteria: factors with p < 0.05 were considered statistically significant. This analysis quantified the influence of parameters on mechanical properties such as Yield Strength, UTS, and % Elongation, enabling a clear ranking of factor importance. [19]

3. Regression Modelling

To establish predictive relationships between input parameters and mechanical properties, multiple linear regression models were developed. These models allow estimation of responses without repeating experiments and facilitate process control and optimisation [20]. A general regression equation is represented as:

$$Y = \beta_0 + \beta_1 X_1 + \beta_2 X_2 + \beta_3 X_3$$

Where:

Y is the response variable (e.g., Yield Strength)

X₁, X₂, and X₃ represent rotational speed, welding speed, and axial load, respectively.

3. Simulations and FSW Parameters

Finite Element Analysis (FEA) using ANSYS Workbench tools provides a powerful and cost-effective method for pre-manufacturing evaluation of these parameters. By simulating the thermal behaviour of the material under varying conditions, it becomes possible to

predict whether sufficient temperature levels are reached for adequate bonding, without causing material degradation or incomplete fusion.

This approach enables the identification of suitable process windows by correlating heat generation with input parameters before actual trials. It also allows the optimisation of parameters while minimising experimental costs and potential material waste. The simulations help ensure that the operating temperature stays within the thermal limits of the base material, such as cast nylon, while promoting strong weld joints. Thus, FEA becomes an essential decision-support tool in selecting parameter combinations that ensure both energy efficiency and joint reliability.[21]

3.1 Finite Element Analysis:

Finite Element Modelling (FEM) is a critical tool for simulating the coupled thermal and mechanical responses during Stir Friction Welding (SFW). The complex interaction between heat generation and plastic deformation makes it challenging to predict weld quality solely through analytical methods. To overcome this, a coupled transient thermal—mechanical analysis was developed using ANSYS, enabling the simulation of time-dependent heating and deformation that occurs due to the tool's motion & axial load. [22] The model helps estimate the temperature fields generated by friction using different combinations of tool rotational speed, welding speed, and axial load, this provides a robust basis for selecting process parameters for adequate bonding without excess thermal buildup. This pre-manufacturing analysis enables better parameter tuning and reduces the need for extensive trial-and-error experiments [21]. Here are the assumptions considered for FEA:

- Unless mentioned, the material is treated as isotropic with uniform properties.
- The mesh is generated with proper connectivity, avoiding any overlaps or voids.
- The stress–strain behaviour is considered nonlinear in nature.
- All bodies are assumed to begin in an undeformed and stress-free condition.
- The initial temperature of the model is set to ambient (26 °C) unless otherwise defined.
- Effects of wear are not included in the analysis.

3.2 CAD Modelling Approach:

The CAD model for the Stir Friction Welding simulation was created in SolidWorks with real-world dimensions suitable for practical production. The workpiece was modelled as a plate measuring 100 mm × 100 mm × 6 mm in thickness, representing a standard cast nylon sheet commonly used in experimental setups. A rotating tool was designed with a tool pin diameter of 6 mm and a pin height of 5.8 mm, shoulder diameter of 25 mm and a height of 15 mm, reflecting the tool designs for controlled heat input and adequate material flow. Simplifications, such as adjusting the tool height, were made to reduce meshing density.

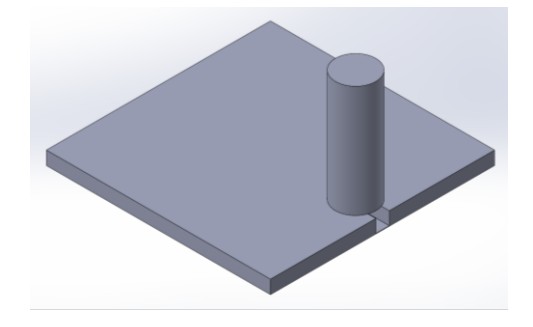


Figure 3.1: CAD Model of FSW Operation

3.3 Simulation

A temperature range of 140–180 °C would be considered best for SFW. The lower limit of 140 °C is chosen because it is well above the glass transition temperature, at which the material becomes sufficiently softened to enable plastic flow without becoming brittle. Temperatures below 140 °C result in inadequate softening, which can lead to poor interfacial bonding and brittle fracture. The upper limit of 180 °C is set to avoid approaching the melting point, where the risk of local melting, thermal degradation, and void formation increases. Operating within a temperature range of 140–180 °C ensures effective material softening for solid-state bonding while maintaining the structural integrity and preventing thermal degradation or splattering [25]. All material properties are taken from Table 2.1.

3.4 Meshing Modelling

Mesh refinement plays a crucial role in ensuring accurate simulation results by improving the solution's convergence toward the actual physical behaviour of the model. The process involves dividing the geometry into smaller elements, where numerical calculations are carried out. A proper balance between mesh density and computational efficiency is crucial for achieving both accuracy and feasibility. [22], [23]

For this analysis, a hexahedral (hexa) mesh was selected due to its superior performance in capturing temperature gradients and deformation behaviour, further refinement were also made. To evaluate whether the mesh is optimal, mesh metrics and convergence are examined in the following sections.

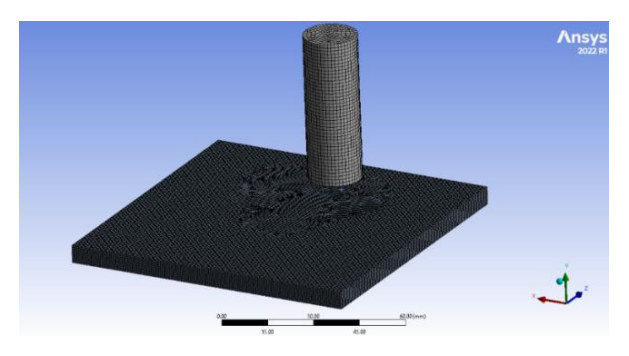


Figure 3.2: Mesh Model of FSW Operation

3.5 Mesh Model Validation

In this study, mesh quality validation was essential to ensure reliable simulation results. A full convergence study—where stability is checked with mesh refinement—was not feasible due to the high computational cost of the non-linear thermomechanical process. Instead, mesh quality was evaluated using metrics such as aspect ratio, element quality, and Jacobian ratio. These indicators helped confirm that the mesh could capture temperature and stress fields in the coupled thermal—mechanical model. [22], [24]

The graphs show that the minimum mesh quality is ~ 1.01 for 1,19,256 elements (71% of the model), indicating well-formed elements. Element quality exceeds 0.75 for 1,32,028 elements (78.5%), ensuring refinement for thermal and structural effects. The Jacobian Ratio is 1 for 1,68,280 elements (96%), reflecting ideal transformation. Orthogonality near 0.75 is seen in 1,28,100 elements (76%), confirming stable alignment. Together, these metrics validate the mesh and enable reliable temperature field prediction across the weld.

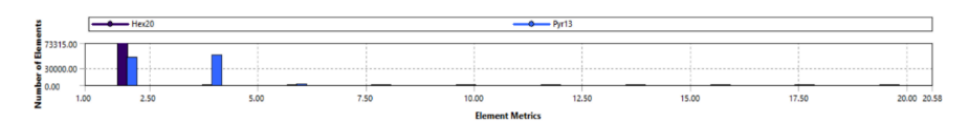


Figure 3.3: Aspect Ratio of the Mesh Model

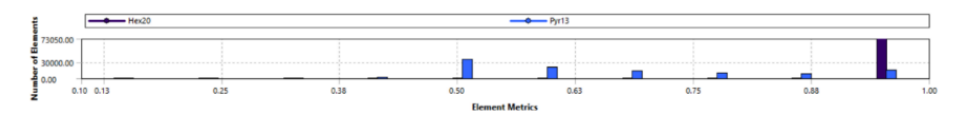


Figure 3.4: Element Quality of the Mesh Model



Figure 3.5: Jacobian Ratio of the Mesh Model

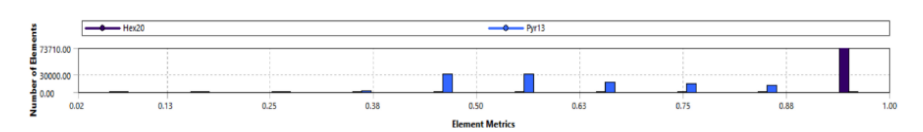


Figure 3.6: Orthogonal Quality of the Mesh Model

3.6 Boundary Condition

- **Thermal Condition**: The initial temperature is set to 26 °C (room temperature).
- Convection condition: the bodies are to have natural convection under stagnant air
- Tool RPM: it is set to 900, 1000, and 1200 to perform the iterations
- Tool velocity: it is set to 15, 20, 25 mm/min according to the iterations
- The load on the tool is set to 130, 140, 150 kgf to accommodate the iterations
- Fixed Support: All the edge faces and the base of the sheet were made fixed

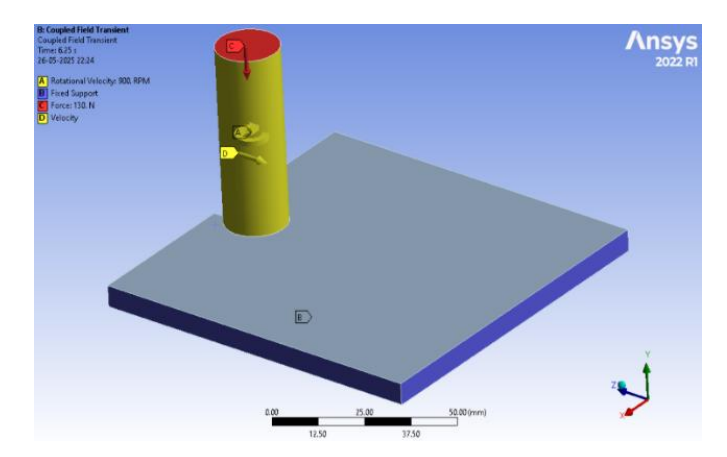


Figure 3.7: ANSYS Simulation Boundary Condition

3.7 Simulation Results and Discussion

Table 3.1: Simulated Weld Pool Temperatures (ANSYS)

S.No	Rotational Speed (RPM)	Weld Speed (mm/min)	Axial Load (Kgf)	Temperature (°C)
1	900	15	130	150.68
2	900	15	140	153.22
3	900	15	150	156.48
4	900	20	130	138.32
5	900	20	140	141.49
6	900	20	150	144.66
7	900	25	130	134.1
8	900	25	140	135.16
9	900	25	150	139.39
10	1000	15	130	156.82
11	1000	15	140	158.54
12	1000	15	150	159.3
13	1000	20	130	142.55
14	1000	20	140	145.72
15	1000	20	150	147.83
16	1000	25	130	136.21
17	1000	25	140	137.27
18	1000	25	150	140.44
19	1200	15	130	166.48
20	1200	15	140	169.14
21	1200	15	150	175.13
22	1200	20	130	149.94
23	1200	20	140	153.07
24	1200	20	150	157.85
25	1200	25	130	143.61
26	1200	25	140	146.78
27	1200	25	150	149.88

Coupled thermal–mechanical ANSYS simulations were performed to study the influence of RPM, welding speed, and axial load on heat generation in SFW. A total of 50 trials were conducted, with 27 parameter sets considered within the target range of 140–180 °C.

Peak temperatures ranged from 134.1 °C to 175.13 °C, confirming sufficient plastic flow for solid-state bonding. These values remain below the 190–220 °C degradation threshold of cast nylon, ensuring minimal risk of molecular breakdown.

The temperature contours show that heat generation is localised around the tool pin and shoulder, gradually spreading into the workpiece. Higher input conditions—specifically, higher RPM and axial load—result in a more intense thermal distribution. For instance:

Higher temperatures closer to the upper end of the safe range are preferred, as they promote better material softening, increased chain mobility, and stronger molecular diffusion across the weld interface—all critical for solid-state bonding in thermoplastics.

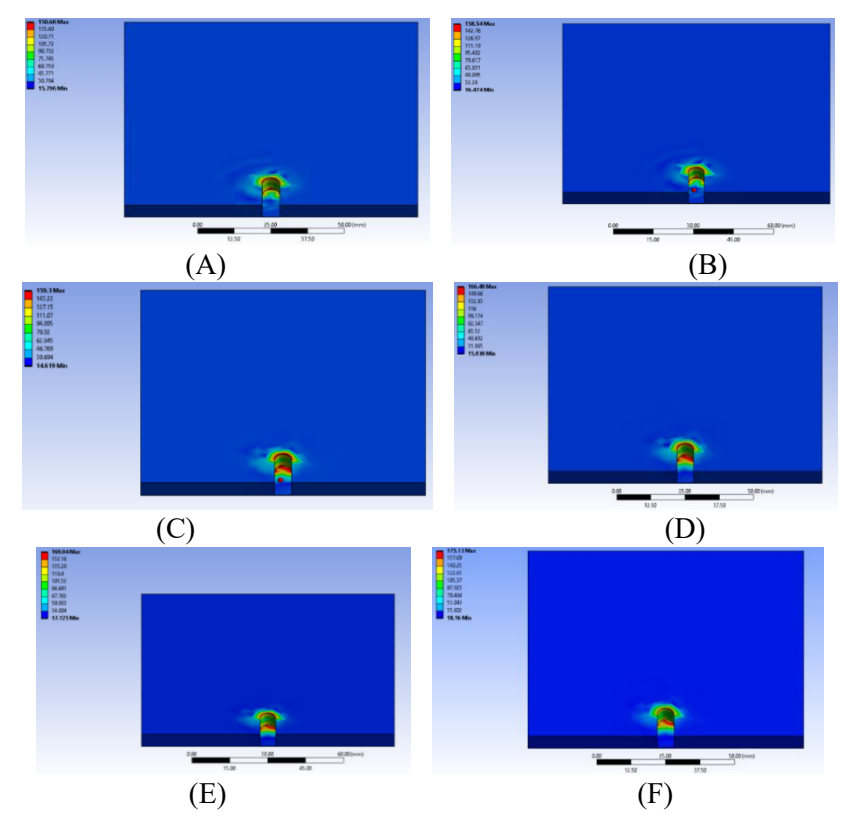


Figure 3.8: ANSYS Simulation Temperature Contour Change with RPM, Load & Weld Speed (A-F)

Simulation contour plots show that temperature and heat flux increase with input energy, particularly at higher RPM and axial loads. This produces deeper, more uniform heating near the tool, improving conduction and softening for stronger welds. In Iterations 12, 19, 20, 21, and 23, tip and shoulder temperatures are nearly equal (Figure 4.8). Iteration 21 (1200 RPM, 15 mm/min, 150 N) is most favourable, with the tool tip slightly hotter than the shoulder, enabling full-depth bonding without exceeding nylon's ~190 °C degradation limit. In contrast, Iterations 1 and 11 show uneven heating, risking weak bonding.

3.8 FSW Parameters & Their Effects

Rotational speed, welding speed, and axial load strongly influence weld quality. Higher RPM generates more frictional heat, raising material temperature to improve plastic flow, mixing, and bonding. Lower welding speeds increase tool interaction and heat input, allowing better softening and denser welds with greater strength, while higher speeds reduce heat and risk weak bonding. Similarly, higher axial loads raise interface pressure, boosting frictional heat and material flow, which helps fill voids, minimize defects, and enhance weld strength and hardness.

Table 3.2: FSW Parameters and Their Levels Based on Simulation Results

Parameter	Level 1	Level 2	Level 3
Rotational Speed (RPM)	900	1000	1200
Weld Speed (mm/min)	15	20	25
Axial Load (Kgf)	130	140	150

4. Results and Discussion

4.1 Tensile test results

Table 4.1: Universal Testing Machine Results of Welded Specimens

S.NO	Rotational Speed (RPM)	Weld Speed (mm/min)	Axial Load (Kgf)	Yield strength (MPa)	UTS (Mpa)	Elongation %
1	900	15	130	37.514	51.705	12.41
2	900	15	140	38.608	52.512	12.86
3	900	15	150	39.645	54.024	13.33
4	900	20	130	34.247	47.205	13.41
5	900	20	140	35.406	48.361	13.96
6	900	20	150	36.772	49.772	14.32
7	900	25	130	32.289	44.505	13.74
8	900	25	140	33.048	45.854	13.37
9	900	25	150	33.701	47.319	13.64
10	1000	15	130	38.602	53.204	14.36
11	1000	15	140	39.521	54.1	14.89
12	1000	15	150	40.217	55.555	15.18
13	1000	20	130	35.336	48.706	15.25
14	1000	20	140	36.272	49.988	14.95
15	1000	20	150	36.947	51.106	14.98
16	1000	25	130	33.377	46.002	15.68
17	1000	25	140	34.773	46.866	15.63
18	1000	25	150	36.258	48.006	15.88
19	1200	15	130	40.778	56.207	14.32
20	1200	15	140	41.931	57.778	14.03
21	1200	15	150	42.838	60.87	13.78
22	1200	20	130	37.514	51.707	15.62
23	1200	20	140	38.404	52.589	15.41
24	1200	20	150	39.681	53.937	15.06
25	1200	25	130	35.554	49.002	15.78
26	1200	25	140	36.558	50.167	15.81
27	1200	25	150	37.652	51.714	15.88



Figure 4.1: FSW's at 900 RPM

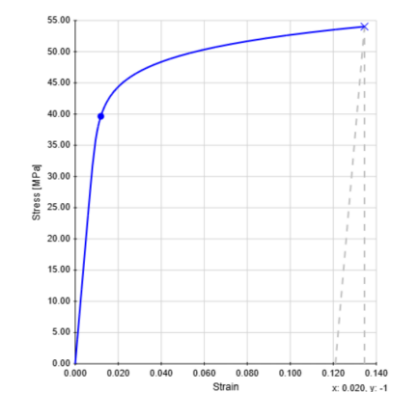


Figure 4.2: Stress-Strain Plot of Best Case at 900 RPM (Specimen 3)



Figure 4.3: FSW's at 1000 RPM

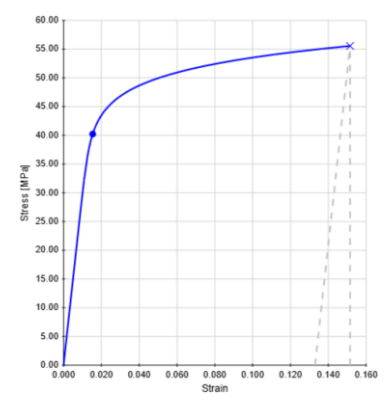


Figure 4.4: Stress-Strain Plot of Best Case at 1000 RPM (Specimen 12)



Figure 4.5: FSW's at 1200 RPM

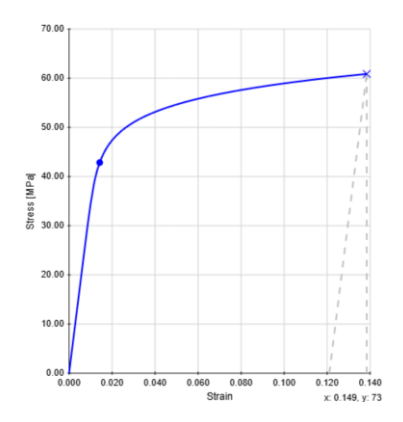


Figure 4.6: Stress-Strain Plot of Best Case at 1200 RPM (Specimen 12)

Experimental results in table 4.1, show clear effects of RPM, welding speed, and axial load on the mechanical properties of friction-stir-welded cast nylon. At constant RPM, higher axial loads improved yield strength, UTS, and elongation, indicating better joint consolidation. For example, at 900 RPM and 15 mm/min, UTS rose from 51.7 MPa to 54 MPa as load increased from 130 N to 150 N. Similar trends at 1000 and 1200 RPM confirm that higher load enhances heat generation and plastic flow. In contrast, raising welding speed from 15 to 25 mm/min reduced strength at lower loads due to insufficient heat & incomplete mixing. These results align with ANSYS simulations, which showed that higher RPM, greater load, and lower weld speeds produced deeper thermal penetration and effective softening, leading to stronger bonding. The strong agreement between experimental and simulated data validates the modelling approach. Overall, optimal weld strength is achieved at 1200 RPM, 140–150 N, and 15–20 mm/min, with Taguchi optimisation applied to refine the best parameter set.

4.2 Rockwell Hardness and Izod Impact Test Results

Table 4.2: Rockwell Hardness-M & Izod Impact Test Results of Welded Specimens

	Rotational	Weld	Axial	Hardı	iess, Roc	kwell M	Toughness
S.NO	Speed (RPM)	Speed (mm/min)	Load (Kgf)	LEFT	MID	RIGHT	(Izod) (J/cm)
1	900	15	130	95.5	95.6	94.1	0.321
2	900	15	140	95.8	96.2	94.4	0.338
3	900	15	150	96.5	97.7	95	0.36
4	900	20	130	94	92.7	92.9	0.317
5	900	20	140	94.3	93.1	93.1	0.338
6	900	20	150	94.6	93.9	93.4	0.356
7	900	25	130	93.4	91.5	92.4	0.306
8	900	25	140	93.6	91.9	92.6	0.307
9	900	25	150	95.9	91	91	0.323
10	1000	15	130	96.1	96.9	94.7	0.382
11	1000	15	140	96.5	97.7	95	0.403
12	1000	15	150	97.3	99.3	95.7	0.422
13	1000	20	130	94.4	93.5	93.2	0.371
14	1000	20	140	94.8	94.2	93.5	0.374
15	1000	20	150	95.2	95	93.9	0.383
16	1000	25	130	93.7	92.1	92.6	0.361
17	1000	25	140	93.8	92.2	92.7	0.366
18	1000	25	150	94.1	92.7	92.9	0.381
19	1200	15	130	96.6	97.8	95.1	0.402
20	1200	15	140	97	99.2	95.9	0.411
21	1200	15	150	98.2	99.2	95.3	0.422
22	1200	20	130	95.5	95.6	94.1	0.404
23	1200	20	140	95.9	96.4	94.5	0.405
24	1200	20	150	96.5	97.6	95	0.406
25	1200	25	130	93.4	94.8	95.3	0.387
26	1200	25	140	93.4	94.8	93.7	0.397
27	1200	25	150	95.4	95.5	94.1	0.411

Table 4.2 shows that Rockwell M hardness and Izod toughness rise with higher RPM and axial load, especially at low welding speeds. At 900 RPM and 15 mm/min, both properties improve steadily with load, and at 1000–1200 RPM the highest values occur at 150 N and 15 mm/min, reflecting optimal softening and mixing. Overall, low weld speed with high RPM and load delivers superior performance, though overlapping results make it difficult to pinpoint the best set. Hence, Taguchi optimisation will be used to determine the optimal combination.

4.3 Taguchi Optimisation Results (L27)

4.3.1 Taguchi Optimisation of Yield Strength (Larger Is Better)

Table 4.3: Response for Means (Yield Strength)

Level	Rotational Speed (RPM)	Weld Speed (mm/min)	Axial Load (Kgf)
1	35.69	39.96	36.13
2	36.81	36.73	37.17
3	38.99	34.80	38.19
Delta	3.30	5.16	2.06
Rank	2	1	3

The Response Table for Means Table 4.3 shows that yield strength increases with an increase in rotational speed from 900 RPM (35.69 MPa) to 1200 RPM (38.99 MPa), while decreasing weld speed from 25 mm/min (34.80 MPa) to 15 mm/min (39.96 MPa) significantly improves yield strength. Axial load also has a positive influence, increasing from 130 Kgf (36.13 MPa) to 150 Kgf (38.19 MPa). The delta values show weld speed (Δ = 5.16) as most influential factor, then rotational speed (Δ = 3.30) & axial load (Δ = 2.06).

Table 4.4: Response for Signal-to-Noise Ratios (Yield Strength)

Level	Rotational Speed (RPM)	Weld Speed (mm/min)	Axial Load (Kgf)
1	31.03	32.03	31.14
2	31.31	31.29	31.38
3	31.80	30.82	31.62
Delta	0.77	1.20	0.48
Rank	2	1	3

The Response Table for Signal-to-Noise Ratios Table 4.4 confirms these findings under the robustness criterion. The highest S/N ratio for weld speed is 32.03 dB at 15 mm/min, for RPM is 31.80 dB at 1200 RPM, and for load is 31.62 dB at 150 Kgf. Here, weld speed ($\Delta = 1.20$) ranks as the most significant factor, followed by RPM ($\Delta = 0.77$) & load ($\Delta = 0.48$).

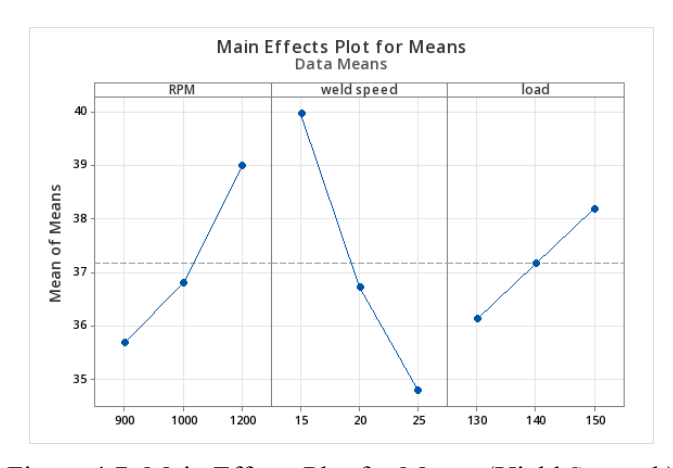


Figure 4.7: Main Effects Plot for Means (Yield Strength)

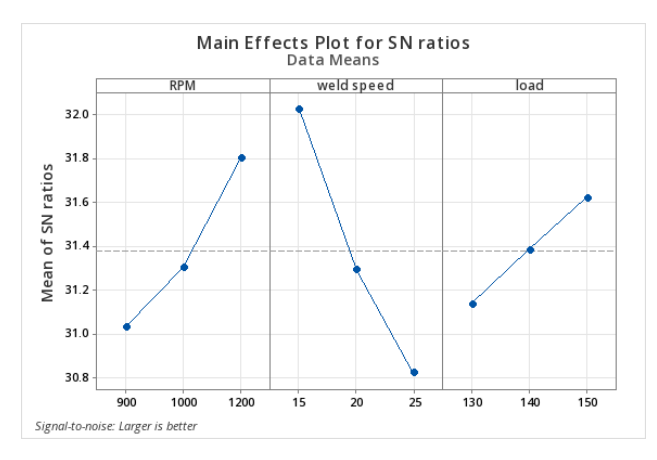


Figure 4.8: Main Effects Plot for Signal-to-Noise Ratios (Yield Strength)

The Main Effects Plot for Means Figure 4.7 demonstrates the trends of the yield strength, increases with RPM, decreases as weld speed increases, and improves moderately with axial load. The Main Effects Plot for S/N Ratios Figure 4.8 confirms that the most robust yield strength is achieved at 1200 RPM, 15 mm/min weld speed, & 150 Kgf axial load.

Regression Equation:

weld speed

load

-0.5160

0.1028

Yield strength (mpa) = 21.75 + 0.010978 RPM - 0.5160 weld speed + 0.1028 load

0.0209

0.0105

	e		C	` .	,
Term	Coef	SE Coef	T-Value	P-Value	VIF
Constant	21.75	1.68	12.94	0.0001	
RPM	0.010978	0.000684	16.04	0.0001	1.00

-24.68

9.83

0.0001

0.0001

1.00

1.00

Table 4.5: Regression Coefficients and Significance (Yield Strength)

Source	DF	Adj SS	Adj MS	F-Value	P-Value
Regression	3	189.470	63.157	320.96	0.0001
RPM	1	50.620	50.620	257.25	0.0001
weld speed	1	119.836	119.836	609.00	0.0001
load	1	19.014	19.014	96.63	0.0001
Error	23	4.526	0.197		
Total	26	193.996			

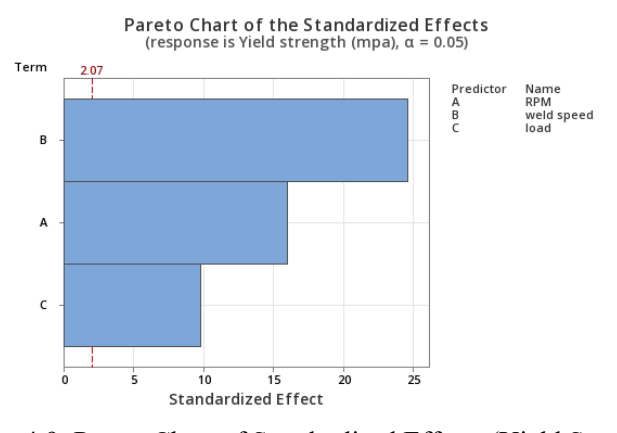


Figure 4.9: Pareto Chart of Standardised Effects (Yield Strength)

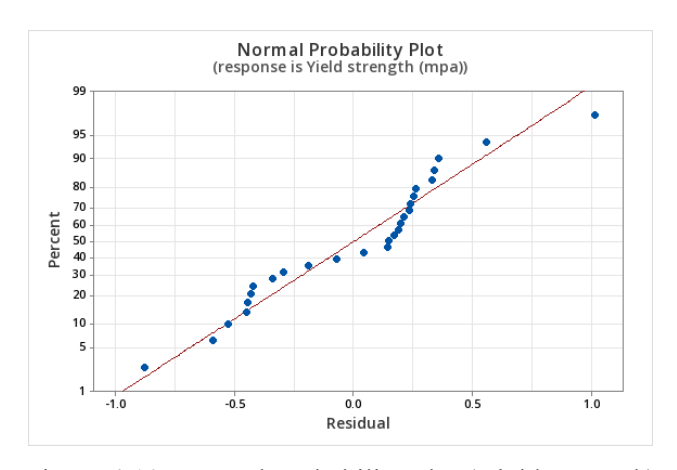


Figure 4.10: Normal Probability Plot (Yield Strength)

The Taguchi analysis identified the optimal process parameters for maximising yield strength, following the "Larger is Better" criterion, which is appropriate here since higher yield strength results in stronger and more durable welds.

From the Means & Signal-to-Noise (S/N) ratio table:

- Weld Speed has the most significant influence (Rank 1), followed by RPM (Rank 2) and Load (Rank 3).
- The best combination for the highest S/N ratio and mean yield strength:

RPM: 1200

Weld Speed: 15 mm/min

o Load: 150 Kgf

The Pareto Chart Figure 4.9 also identifies weld speed as the most significant factor, followed by RPM and load, supporting the above findings.

The Normal Probability Plot Figure 4.10 for yield strength shows that most of the data points follow the straight line closely, indicating good normality in general. However, slight deviations are observed in the middle & end sections of the plot, where some points deviate from the line. This suggests mild non-linearity or variability in specific ranges; however, the residuals remain reasonably distributed, confirming the overall model reliability.

4.3.2 Taguchi Optimisation of Ultimate Tensile Strength (Larger Is Better)

Level	Rotational Speed (RPM)	Weld Speed (mm/min)	Axial Load (Kgf)
1	49.03	55.11	49.80
2	50.39	50.37	50.91
3	53.77	47.72	52.48
Delta	4.75	7.39	2.67
Rank	2	1	3

Table 4.7: Response for Means (UTS)

The Response Table for Means Table 4.9 indicates that ultimate tensile strength increases as rotational speed rises from 900 RPM (49.03 MPa) to 1200 RPM (53.77 MPa). Weld speed has a pronounced effect — decreasing from 25 mm/min (47.72 MPa) to 15 mm/min (55.11 MPa) significantly improves UTS. Axial load also contributes positively, with an increase from 130 Kgf (49.80 MPa) to 150 Kgf (52.48 MPa). The delta values confirm that weld speed ($\Delta = 7.39$) is the most influential factor, followed by rotational speed ($\Delta = 4.75$) and axial load ($\Delta = 2.67$).

Level	Rotational Speed (RPM)	Weld Speed (mm/min)	Axial Load (Kgf)
1	33.79	34.81	33.92
2	34.03	34.04	34.12
3	34.59	33.56	34.38
Delta	0.80	1.25	0.45
Rank	2	1	3

Table 4.8: Response for Signal-to-Noise Ratios (UTS)

The Response Table for Signal-to-Noise Ratios Table 4.10 shows a similar ranking, with weld speed again taking Rank 1 (Δ = 1.25), followed by RPM (Δ = 0.80) and axial load (Δ = 0.45). The highest S/N ratio for UTS is achieved at 1200 RPM, 15 mm/min weld speed, and 150 Kgf load, confirming this as the optimal parameter combination.



Figure 4.11: Main Effects Plot for Means (UTS)

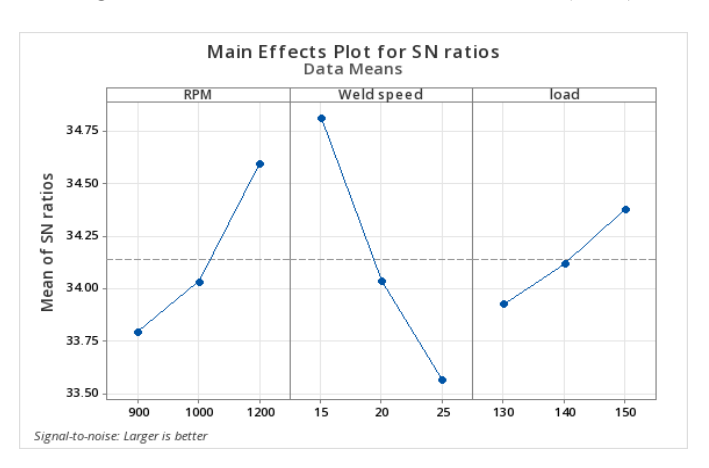


Figure 4.12: Main Effects Plot for Means for Signal-to-Noise Ratios (UTS)

The Main Effects Plot for Means Figure 4.11 visually illustrates that UTS improves steadily with increasing RPM, increases sharply when weld speed is reduced, and shows moderate improvement with higher axial load. The Main Effects Plot for S/N Ratios Figure 4.12 supports these findings, indicating that the chosen optimum also yields the most consistent and robust results.

Regression Equation:

UTS = 30.63 + 0.01598 RPM - 0.7391 Weld speed + 0.1337 load

Table 4.9: Regression Coefficients and Significance (UTS)

Term	Coef	SE Coef	T-Value	P-Value	VIF
Constant	30.63	2.69	11.39	0.0001	
RPM	0.01598	0.00110	14.59	0.0001	1.00
Weld speed	-0.7391	0.0335	-22.09	0.0001	1.00
load	0.1337	0.0167	7.99	0.0001	1.00

Table 4.10: Analysis of Variance (ANOVA) (UTS)

Source	DF	Adj SS	Adj MS	F-Value	P-Value
Regression	3	385.18	128.394	254.89	0.0001
RPM	1	107.19	107.194	212.80	0.0001
Weld speed	1	245.83	245.828	488.01	0.0001
load	1	32.16	32.160	63.84	0.0001
Error	23	11.59	0.504		
Total	26	396.77			

Pareto Chart of the Standardized Effects
(response is UTS, α = 0.05)

Term

207

Predictor Name
A RPM
A RPM
B Weld speed load

C

C

Standardized Effect

Figure 4.13: Pareto chart of Standardised Effects (UTS)

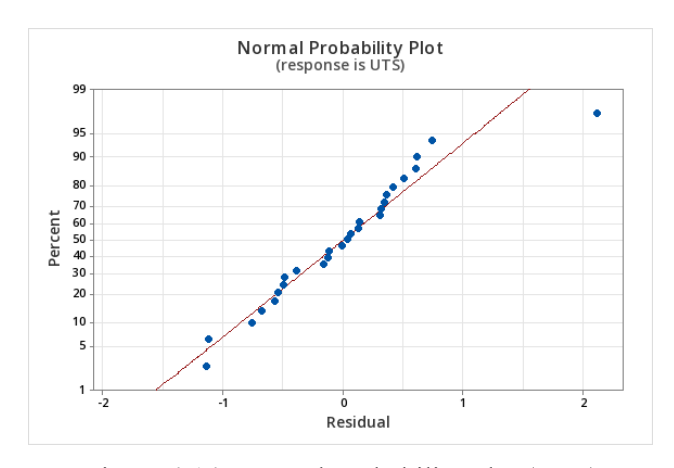


Figure 4.14: Normal Probability Plot (UTS)

The Taguchi analysis was applied to optimise UTS using the "Larger is Better" approach, which is appropriate since higher UTS improves joint strength and load-carrying capacity. From the Mean Response Table & Signal-to-Noise (S/N) ratio table:

• Weld Speed ranks as the most significant factor (Rank 1), followed by RPM (Rank 2) and Load (Rank 3).

• The highest S/N ratios were achieved at:

RPM: 1200

Weld Speed: 15 mm/min

Load: 150 kgf

This combination maximises UTS across both S/N ratios & means, making it the optimal solution.

The Regression Analysis further confirms that weld speed has the most significant influence, followed by RPM and load, which aligns with the Taguchi ranking.

The Normal Probability Plot of residuals UTS Figure 4.14 shows that most points are almost perfectly aligned with the straight line, confirming that the residuals are normally distributed. Only a single point at the far end deviates slightly, which is acceptable and common in experimental data. This indicates that the regression model is statistically valid, highly reliable, and capable of accurately predicting UTS within the tested range.

4.3.3 Taguchi Optimisation of Hardness (Larger Is Better)

Level	Rotational Speed (RPM)	Weld Speed (mm/min)	Axial Load (Kgf)
1	93.93	96.46	94.35
2	94.58	94.47	94.67
3	95.77	93.35	95.26
Delta	1.84	3.10	0.90
Rank	2	1	3

Table 4.11: Response for Means (Hardness)

The Response Table for Means Table 4.15 shows that Hardness increases with rising rotational speed, from 93.93 HR at 900 RPM to 95.77 HR at 1200 RPM. Weld speed has the most prominent influence, with a reduction from 25 mm/min (93.35 HR) to 15 mm/min (96.46 HR), leading to the highest hardness. Axial load has a more minor but positive effect, increasing from 130 Kgf (94.35 HR) to 150 Kgf (95.26 HR). The delta values confirm the ranking: weld speed (Δ = 3.10, Rank 1), RPM (Δ = 1.84, Rank 2), and axial load (Δ = 0.90, Rank 3).

Level	Rotational Speed (RPM)	Weld Speed (mm/min)	Axial Load (Kgf)
1	39.46	39.69	39.49
2	39.51	39.51	39.52
3	39.62	39.40	39.58
Delta	0.17	0.28	0.08
Rank	2	1	3

Table 4.12: Response for Signal-to-Noise Ratios (Hardness)

The Response Table for Signal-to-Noise Ratios Table 4.16 mirrors this order, with weld speed again in Rank 1 ($\Delta = 0.28$), followed by RPM ($\Delta = 0.17$) and axial load ($\Delta = 0.08$). The highest S/N ratio for hardness was obtained at 1200 RPM, 15 mm/min weld speed, and 150 Kgf load, indicating optimal robustness.

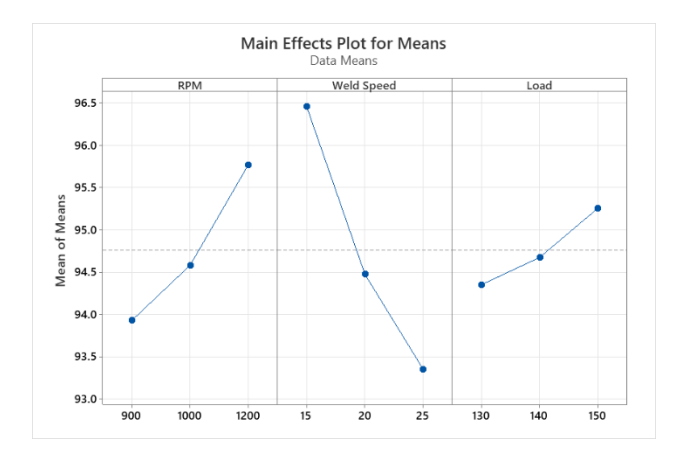


Figure 4.15: Main Effects Plot for Means (Hardness)

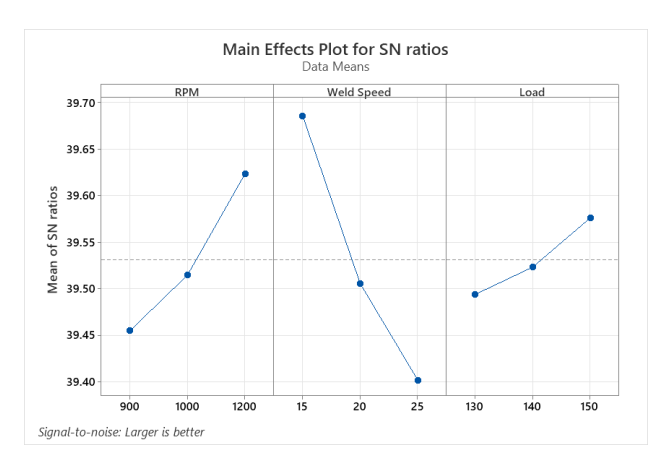


Figure 4.16: Main Effects Plot for Signal-to-Noise Ratios (Hardness)

The Main Effects Plot for Means in Figure 4.15 shows that Hardness improves with increasing RPM, rises sharply when weld speed is reduced, and gains moderately with higher axial load. Similarly, Figure 4.16 illustrates that UTS increases with higher RPM, improves significantly at lower weld speed, and shows additional enhancement at higher axial load. Together, these plots confirm that welding speed is the most influential parameter, followed by rotational speed and axial load, in determining the strength of the joints.

Regression Equation

Hardness = 88.33 + 0.006108 RPM - 0.3104 Weld Speed + 0.04519 Load

Table 4.13: Regression Coefficients and Significance (Hardness)

Term	Coef	SE Coef	T-Value	P-Value	VIF
Constant	88.33	1.48	59.75	0.0001	
RPM	0.006108	0.000602	10.15	0.0001	1.00
Weld speed	-0.3104	0.0184	-16.88	0.0001	1.00
Load	0.04519	0.00920	4.91	0.0001	1.00

Table 4.14: Analysis of Variance (ANOVA) (Hardness)

Source	DF	Adj SS	Adj MS	F-Value	P-Value
Regression	3	62.695	20.8984	137.31	0.0001
RPM	1	15.672	15.6716	102.97	0.0001
Weld speed	1	43.348	43.3484	284.81	0.0001
Load	1	3.675	3.6751	24.15	0.0001
Error	23	3.501	0.1522		
Total	26	66.196			

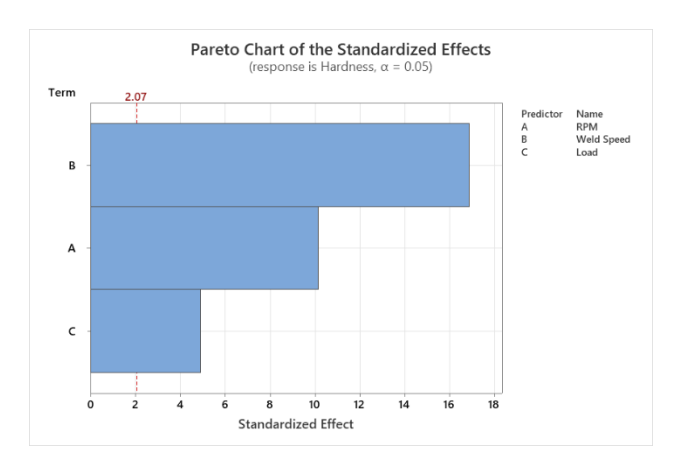


Figure 4.17: Pareto Chart of Standardised Effects (Hardness)

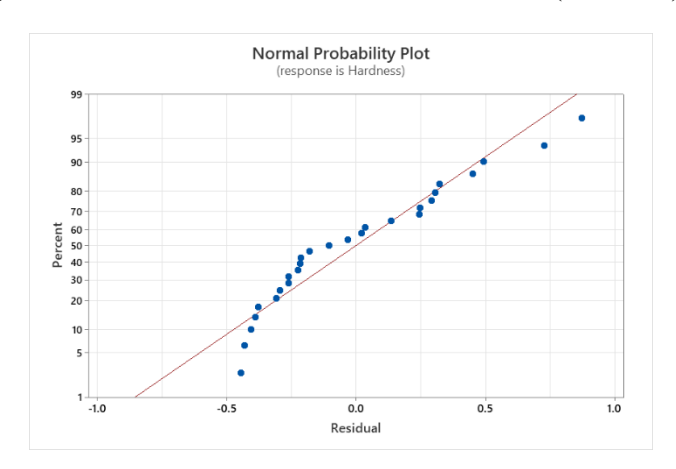


Figure 4.18: Normal Probability Plot (Hardness)

Taguchi optimisation was performed for hardness using the "Larger is Better" approach, as higher weld hardness improves wear resistance and surface durability.

From the Mean Response Table & Signal-to-Noise (S/N) ratio table:

- Weld Speed had the strongest effect (Rank 1), followed by RPM (Rank 2) & Load (Rank 3).
- Optimal parameters for maximum hardness:

RPM: 1200

• Weld Speed: 15 mm/min

Load: 150 kgf

The Regression Analysis further verifies that weld speed is the most influential factor, followed by RPM and load, consistent with Taguchi results.

The Normal Probability Plot for Hardness Figure 4.18 shows more noticeable deviations at the initial and end sections of the plot, with points scattered away from the line in these regions. However, the mid-range values lie closely along the straight line, suggesting that most of the residuals near the average values are normally distributed. While there is some variability at the extremes, the plot generally supports the model's statistical validity for the majority of the data range.

Higher weld hardness is beneficial for weld quality. According to welding references, the weld hardness should ideally be 15 points higher than or equal to the base material to ensure proper weld strength and wear resistance until it enters the brittle region [35]. The optimised parameter set achieved hardness values near or above this threshold, indicating acceptable and enhanced weld quality.

4.3.4 Taguchi Optimisation of Toughness (Larger Is Better)

Level	Rotational Speed (RPM)	Weld Speed (mm/min)	Axial Load (Kgf)
1	0.3296	0.3846	0.3612
2	0.3826	0.3727	0.3710
3	0.4050	0.3599	0.3849
Delta	0.0754	0.0247	0.0237
Rank	1	2	3

Table 4.15: Response Table for Means (Toughness)

The Response Table for Means Table 4.21 shows that toughness increases notably with higher rotational speed, from 0.3296 J/cm at 900 RPM to 0.4050 J/cm at 1200 RPM. Weld speed has a more minor but measurable effect, with the highest toughness achieved at 15 mm/min (0.3846 J/cm) and the lowest at 25 mm/min (0.3599 J/cm). Axial load shows the least variation, increasing from 0.3612 J/cm at 130 Kgf to 0.3849 J/cm at 150 Kgf. The delta values confirm that RPM (Δ = 0.0754) is the most significant factor, followed by weld speed (Δ = 0.0247) and axial load (Δ = 0.0237).

Level	Rotational Speed (RPM)	Weld Speed (mm/min)	Axial Load (Kgf)
1	-9.655	-8.338	-8.888
2	-8.355	-8.602	-8.652
3	-7.853	-8.924	-8.324
Delta	1.802	0.585	0.563
Rank	1	2	3

Table 4.16: Response for Signal-to-Noise Ratios (Toughness)

The Response Table for Signal-to-Noise Ratios Table 4.22 supports this ranking, with RPM again as the most dominant factor (Δ = 1.802), followed by weld speed (Δ = 0.585) and load (Δ = 0.563). The optimal combination for maximum toughness is 1200 RPM, 15 mm/min weld speed, and 150 Kgf load.

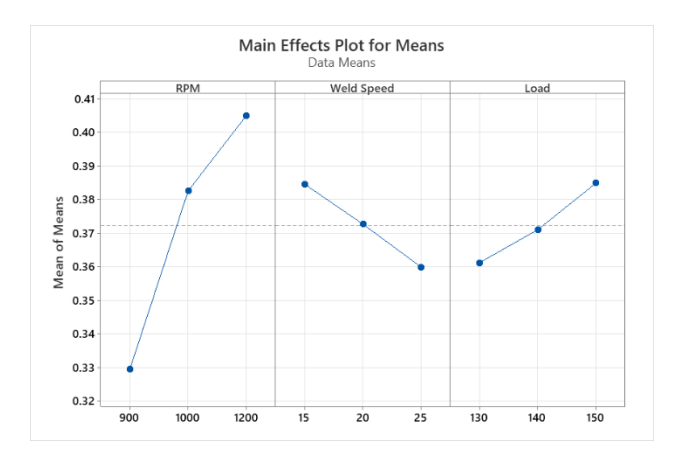


Figure 4.19: Main Effects Plot for Means (Toughness)

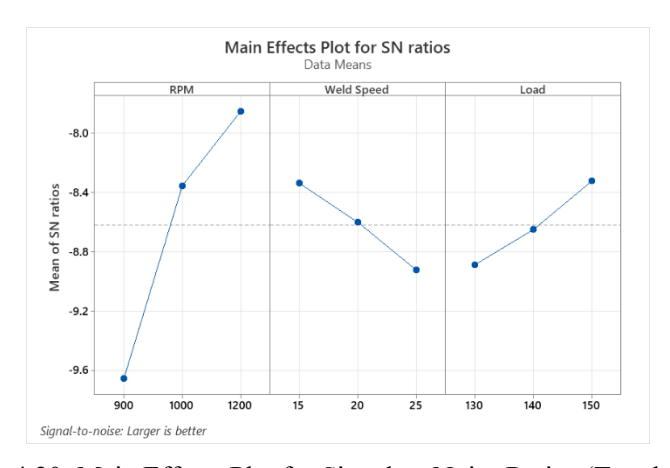


Figure 4.20: Main Effects Plot for Signal-to-Noise Ratios (Toughness)

The Main Effects Plot for Means in Figure 4.19 shows that toughness increases with rising RPM, improves significantly when weld speed is reduced, and gains further with higher axial load. The Main Effects Plot for S/N Ratios in Figure 4.20 confirms these observations.

Regression Equation

Toughness = 0.0167 + 0.000232 RPM - 0.002467 Weld Speed + 0.001183 Load

Table 4.17: Regression Coefficients and Significance (Toughness)

Term	Coef	SE Coef	T-Value	P-Value	VIF
Constant	0.0167	0.0613	0.27	0.7870	
RPM	0.000232	0.000025	9.28	0.0001	1.00
Weld speed	-0.002467	0.000763	-3.23	0.0040	1.00
Load	0.001183	0.000381	3.10	0.0050	1.00

Table 4.18: Analysis of Variance (ANOVA) (Toughness)

Source	DF	Adj SS	Adj MS	F-Value	P-Value
Regression	3	0.027784	0.009261	35.40	0.0001
RPM	1	0.022526	0.022526	86.09	0.0001
Weld speed	1	0.002738	0.002738	10.46	0.0040
Load	1	0.002520	0.002520	9.63	0.0050
Error	23	0.006018	0.000262		
Total	26	0.033802			

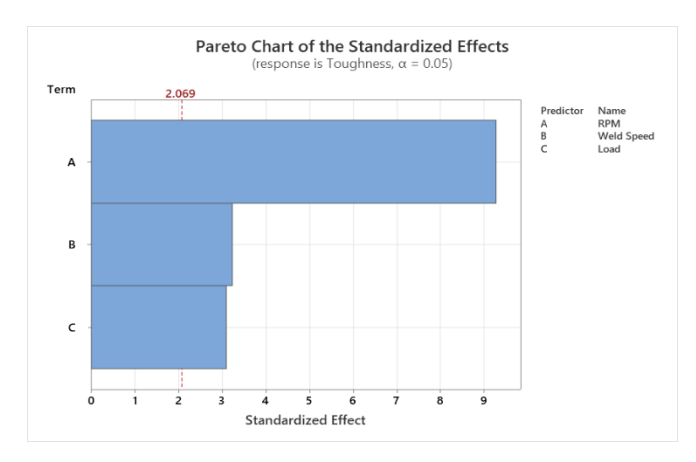


Figure 4.21: Pareto Chart of Standardised Effects (Toughness)

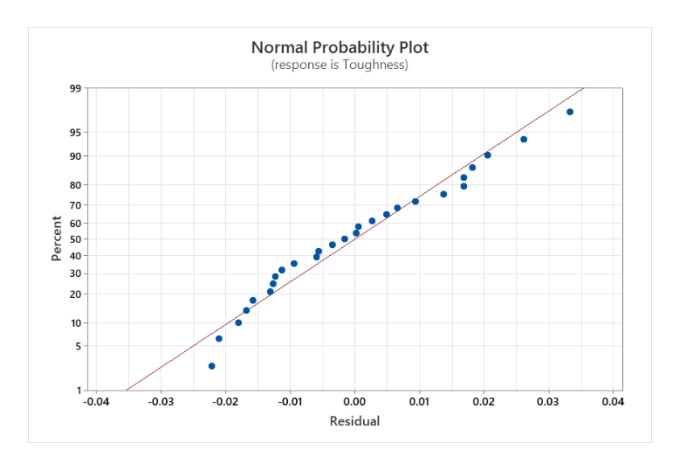


Figure 4.22: Normal Probability Plot (Toughness)

Taguchi optimisation was performed to maximise toughness using the "Larger is Better" approach, as higher toughness improves the weld's resistance to impact and brittle failure. From the Signal-to-Noise (S/N) ratio table:

- RPM had the highest influence on toughness (Rank 1), followed by weld speed (Rank 2) and load (Rank 3).
- The optimal parameter settings for maximum toughness:

o **RPM:** 1200

o Weld Speed: 15 mm/min

Load: 150 kgf

The Mean Response Table confirmed the same optimal settings, showing that higher RPM consistently improves toughness.

The Regression Analysis also confirmed that RPM is the most significant factor, followed by weld speed and load. The R² value of 82.20% indicates moderate model accuracy—slightly lower than for other properties, such as yield strength or hardness—but still acceptable.

Notably, the Normal Probability Plot of residuals showed points closely following the straight line, indicating that the residuals are normally distributed and that the regression model is statistically valid, despite a moderate R² value. This confirms the model's reliability for predicting toughness within the tested parameter range. Although Taguchi optimisation still successfully identified the best parameters for maximising toughness. Higher RPM improves heat input and material mixing, which enhances ductility and energy absorption during impact.

4.4 Induction-based Friction Stir Welding Results

To evaluate the effect of induction heating on stir friction welding (SFW), a focused testing strategy is adopted instead of repeating the full parameter matrix. Induction supports controlled melting, which may stay below melting or risk degradation depending on parameters. Earlier optimisation showed welding speed is the most critical factor, as lower speeds improve bonding through higher heat input.

The best tensile strength condition—1200 RPM and 150 kgf axial load—is taken as the baseline since no degradation was observed. Induction heating will raise tool temperature to 70 °C, and weld speed will be increased in 2.5 mm/min increments from this setting to study its effect on bonding and strength.

This approach highlights how induction-assisted SFW can achieve higher weld speeds without loss of quality. It also addresses the impractically slow 15 mm/min speed used earlier, showing how induction can improve both joint integrity and production efficiency for industrial use.

S.NO	Weld Speed (mm/min)	Yield strength (MPa)	UTS (MPa)	Elongation %	Toughness (J/cm)
1	15	32.91	39.19	6.18	0.152
2	17.5	38.25	48.01	9.64	0.278
3	20	44.91	58.19	13.87	0.411
4	22.5	49.51	65.44	16.22	0.499
5	25	50.76	66.74	16.47	0.513
6	27.5	49.2	64.86	16.61	0.521
7	30	47.84	60.48	16.01	0.484
8	32.5	43.19	55.27	14.38	0.415
9	35	42.07	52.02	13.65	0.381

Table 4.19: Induction-Based FSW Test Results

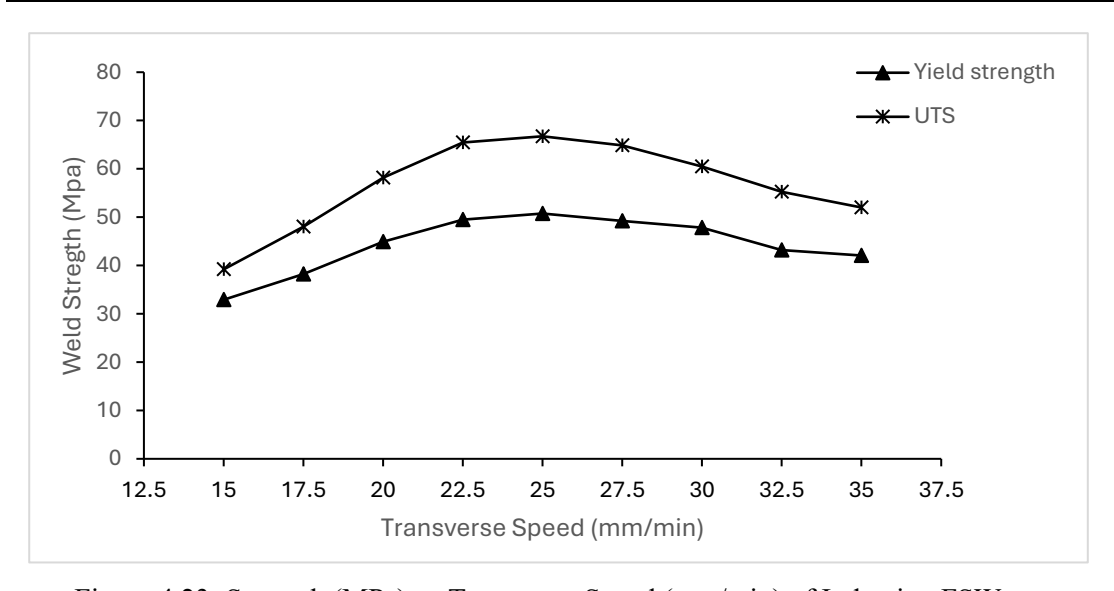


Figure 4.23: Strength (MPa) vs Transverse Speed (mm/min) of Induction FSW

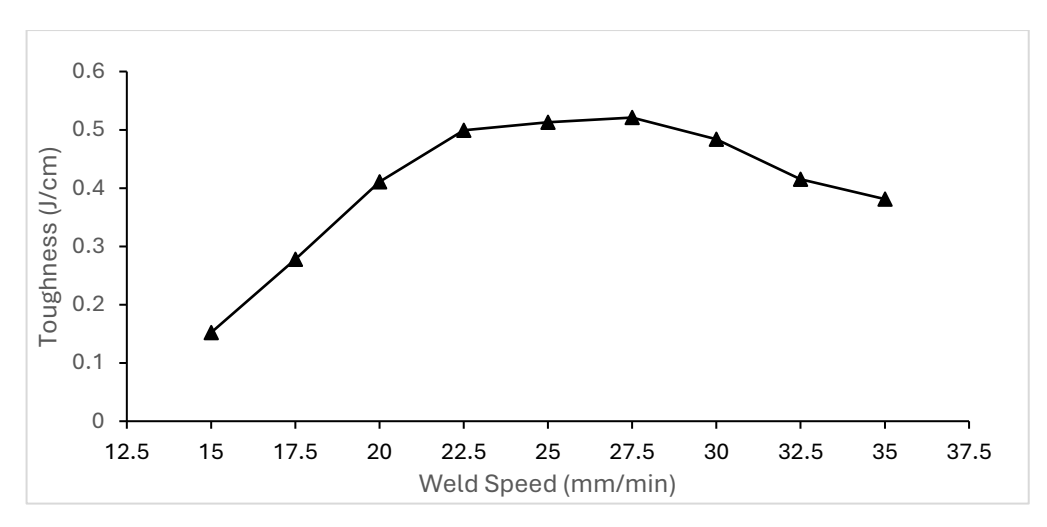


Figure 4.24: Toughness (J/cm) vs Transverse Speed (mm/min) of Induction FSW

The results of the induction-assisted stir friction welding (SFW) process across varying welding speeds clearly show how mechanical performance improves with controlled heat input and optimised welding parameters.

From Figure 4.23, at low welding speeds (15–17.5 mm/min), both yield strength and UTS remain low, with a small gap between them, low elongation, and very low toughness, indicating brittle behaviour likely due to thermal degradation.

As speed increases to the 20–25 mm/min range, mechanical properties improve significantly. Peak performance occurs at 25 mm/min, showing the highest strength, high elongation, and a wide UTS-yield gap, indicating optimal softening and strong, ductile joints without signs of degradation.

Beyond 27.5 mm/min, strength and toughness begin to slightly decline. However, toughness reaches its peak here, even with a minor strength drop, reflecting stable ductility. At the highest speed, yield strength and UTS drop by about 15–20%, and toughness reduces by nearly 25% compared to peak values. This suggests insufficient heat input at higher speeds, leading to weaker bonding. Still, moderate UTS—yield gaps and decent elongation indicate failure is less brittle than at low speeds.

4.4.1 Comparison of Convectional FSW & Induction Based FSW

Table 4.20: Comparable Non-Induction and Induction FSW Results

	Non-Induction			Induction (70 °C)			
Test No	21	24	27	1	3	5	7
Rotational Speed (RPM)	1200	1200	1200	1200	1200	1200	1200
Axial Load (Kgf)	150	150	150	150	150	150	150
Weld Speed (mm/min)	15	20	25	15	20	25	30
Yield strength (MPa)	42.838	39.681	37.652	32.91	44.91	50.76	47.84
UTS (Mpa)	60.87	53.937	51.714	39.19	58.19	66.74	60.48
Elongation %	13.78	15.06	15.88	6.18	13.87	16.47	16.01
Izod Impact (J/cm)	0.422	0.406	0.411	0.152	0.411	0.513	0.484

When comparing induction-assisted SFW with the non-induction process at identical welding speeds, induction showed clear effects on weld performance.

At 15 mm/min, the non-induction weld delivered the best results of all trials: YS 42.84 MPa, UTS 60.87 MPa, elongation >12%, and toughness 0.422 J/cm, with ANSYS predicting 175.13°C at the weld zone. With induction preheating of 70°C, the weld temperature rose above 200°C, exceeding nylon's stability limit. This excessive heating degraded the material, reducing properties to YS 32.91 MPa, UTS 39.19 MPa, elongation 6.18%, & toughness 0.152 J/cm, indicating brittle fracture caused by thermal overexposure. At 20 mm/min, induction started to show its benefits. The non-induction weld gave UTS 53.94 MPa and elongation 15.06%, while the induction-assisted weld improved to UTS 58.19 MPa, YS 44.91 MPa, and toughness 0.411 J/cm. Predicted weld temperatures were 157.85°C (non-induction) and under 190°C (induction). At this speed, the higher travel rate reduced heat per unit length, preventing excessive accumulation & allowing the weld to benefit from steady preheating. The result was stronger joints with ductility and toughness. At 30 mm/min, the benefits of induction were most pronounced. Non-induction welding achieved UTS 51.71 MPa and YS 37.65 MPa, with a predicted weld temperature of 149.88°C. Induction raised the weld zone to ~175–180°C, similar to the non-induction case at 15 mm/min, but without causing degradation due to reduced exposure time. This preheating, improved stress relaxation and molecular mobility during cooling. As a result, induction achieved UTS 60.48 MPa, YS 47.84 MPa, and toughness 0.521 J/cm, surpassing the best non-induction performance while doubling the production rate.

At 25 mm/min, induction reached peak performance. Welds showed YS 50.76 MPa, UTS 66.74 MPa, elongation 16.47%, and toughness 0.513 J/cm, outperforming the best non-induction result (at 15 mm/min) while running 66.7% faster. This suggests a thermal sweet spot near 180°C, where the material softened sufficiently for strong bonding but avoided degradation, giving simultaneous gains in strength and toughness.

In summary, induction at very low speeds (>200°C) causes overheating and degradation, but at moderate—high speeds it enhances joint strength, ductility, toughness, productivity. The controlled heat input acts as in-situ annealing, stabilizing the weld zone, improving stress distribution, & making the process faster, more reliable manufacturing.

5. Conclusion

- ANSYS simulations defined safe temperature windows, showing the weld zone stayed within the 140–180 °C softening range for 27 among the 50 above glass transition but below the solidus (~120 °C) and liquidus (~200 °C) of Cast Nylon. This enabled plastic flow without melting or degradation, and close agreement with experiments validated FEA as a reliable tool for parameter selection.
- In non-induction trials, the trend of the parameters—rotational speed (900, 1000, 1200 RPM), welding speed (15, 20, 25 mm/min), and axial load (130, 140, 150 Kgf), showed higher RPM improved heat generation, lower speeds encouraged better mixing, & higher loads enhanced bonding, though heat imbalance at higher speeds occasionally led to brittleness. Taguchi L27 (ANOVA and S/N ratio) analysis identified the optimum set of 1200 RPM, 15 mm/min, and 150 kgf, achieving maximum yield strength (42.838 MPa), UTS (60.87 MPa), hardness, and toughness (0.422 J/cm).
- With induction assistance, localized preheating offsets the usual strength loss at higher welding speeds. At 30 mm/min, induction-assisted welds matched the strength of non-induction welds at 15 mm/min, effectively doubling productivity. At 25 mm/min, induction-assisted joints achieved properties close to the base material (Yield strength: 50.76 Mpa, Ultimate strength: 66.74 Mpa & Toughness 0.513 J/cm), which was

- unattainable without preheating. This highlighted induction as a tool to improve weld efficiency while preserving integrity.
- The induction system also enabled in-situ annealing through continuous heating of the
 weld zone. This effect promoted stress relaxation, increased molecular mobility, and
 reduced residual stresses. The resulting joints showed higher ductility, uniformity, and
 reliability, while avoiding localized brittleness often seen in thermoplastics.

REFERENCE

- [1] M. A. R. Pereira, I. Galvão, J. D. Costa, A. M. Amaro, and R. M. Leal, "Joining of Fibre-Reinforced Thermoplastic Polymer Composites by Friction Stir Welding—A Review," Applied Sciences, vol. 12, no. 5, p. 2744, Mar. 2022, doi: https://doi.org/10.3390/app12052744.
- [2] "Figure 1: Applications of friction stir welding /processing," ResearchGate, 2023. https://www.researchgate.net/Figure/Applications-of-friction-stir-welding-processing Figure 1 377758648.
- [3] Bandari Vijendra and A. Sharma, "Induction heated tool assisted friction-stir welding (i-FSW): A novel hybrid process for joining of thermoplastics," Journal of Manufacturing Processes, vol. ,20, pp. 234–244, Jul. 2015, doi: https://doi.org/10.1016/j.jmapro.2015.07.005.
- [4] "Friction-based welding processes: friction welding and friction stir welding," Journal of Adhesion Science and Technology, 2020, doi: https://doi.org/10.1080//01694243.2020.1780716.
- [5] K. de Naoum and J. Schadegg, "7 Properties of Nylon: Everything you Need to Know," Xometry.com, Jun. 23, 2022. https://www.xometry.com/resources/materials/properties-of-nylon/
- [6] "Overview of materials for Nylon 6, Cast," Matweb.com, 2025. https://matweb.com/search/DataSheet.aspx?MatGUID=8d78f3cfcb6f49d595896ce6ce6a2ef1&ckck=1
- [7] "Nylacast PA6C Cast Nylon 6," Matweb.com, 2025. https://www.matweb.com/search/datasheet.aspx?matguid=ec8edbd5f253414695bda84daaaebd29&ckc k=1
- [8] D. McClements, "High-Speed Steel: Definition, Compositions, Properties, and Uses," *Xometry.com*, Oct. 05, 2023. https://www.xometry.com/resources/materials/high-speed-steel/
- [9] in DFU, "Arduino Stack Exchange," Arduino Stack Exchange, Apr. 28, 2020. https://arduino.stackexchange.com/questions/75238/put-arduino-in-dfu-mode-no-rst-pin.
- [10] "DS18B20 PRO MINI," Arduino Forum, Oct. 20, 2018. https://forum.arduino.cc/t/ds18b20-pro-mini/552006.
- [11] "Arduino coin counter project," Arduino Forum, Sep. 15, 2024. https://forum.arduino.cc/t/arduino-coin-counter-project/1301807.
- [12] "Hot Air Gun Heaters Dovy Electricals," Dovy Electricals, Mar. 11, 2025. https://dovyelectricals.com/product/hot-air-gun-heaters/.
- [13] "How to connect everything together properly?" Arduino Forum, Aug. 28, 2021. https://forum.arduino.cc/t/how-to-connect-everything-together-properly/899985.
- [14] Hà Trần Mạnh, "BS EN 12814-2-2021," Scribd, https://www.scribd.com/document/658591959/BS-EN-12814-2-2021.
- [15] E. Team, "COVID-19 Situation: Six Sigma Ongoing Training Announcements," SixSigma.us, Oct. 08, 2024. https://www.6sigma.us/process-design/taguchi-method/.
- [16] Saheed Olanisebe, J. Abu, S. A. Lawal, E. Egbe, and Oyewole Adedipe, "Morphology and Optimisation of Impact Energy of Weldment of High Strength Low Alloy Steel," FUOYE Journal of Engineering and Technology, vol. 1, no. 1, Sep. 2016, doi: https://doi.org/10.46792/fuoyejet.v1i1.27.
- [17] E. Team, "COVID-19 Situation: Six Sigma Ongoing Training Announcements," SixSigma.us, Oct. 08, 2024. https://www.6sigma.us/process-design/taguchi-method/.
- [18] "Methods and formulas for Analyze Taguchi Design," Minitab.com, 2025. https://support.minitab.com/en-us/minitab/help-and-how-to/statistical-modeling/doe/how-to/taguchi/analyze-taguchi-design/methods-and-formulas/methods-and-formulas/.
- [19] "Analysis of variance table for Analyze Taguchi Design," Minitab.com, 2025. https://support.minitab.com/en-us/minitab/help-and-how-to/statistical-modeling/doe/how-to/taguchi/analyze-taguchi-design/interpret-the-results/all-statistics-and-graphs/analysis-of-variance-table/.
- [20] "Model summary table for Analyze Taguchi Design," Minitab.com, 2025. https://support.minitab.com/en-us/minitab/help-and-how-to/statistical-modeling/doe/how-

- to/taguchi/analyze-taguchi-design/interpret-the-results/all-statistics-and-graphs/model-summary-table/.
- [21] "What is Finite Element Analysis (FEA)? | Ansys," Ansys.com, 2024 https://www.ansys.com/simulation-topics/what-is-finite-elementanalysis#:~:text=FEA%20models%20depend%20on%20the,FEA%20produce%20accurate%2 0insights%20out.
- [22] "Get in Touch | Ansys," Ansys.com, 2021 https://www.ansys.com/company-information/ansyssimulation-software?&utm_campaign=brand&utm_medium=paidsearch&utm_source=google&utm_content=digital_simulation_copr15en_contact_contactus_engineeringsoftware-generalbrandsearch_1a_en_global|145854623758|643896971461|&campaignid=7013g000000cXB4A AM&utm_term=ansys%20engineering%20simulation%20software&gad_source=1&gclid=CjwKCAi A9IC6BhA3EiwAsbltOG1IXvg70zUU8bqbXmdulaOcCNhsoLhtkAo6YP30iezC9WjTxOBV_RoCoF kQAvD_BwE.
- [23] H. Mesh, "Hexahedral Mesh vs. Tetrahedral: Comparing High-Quality Meshing," Cadence.com, Nov.04, 2022. https://resources.system-analysis.cadence.com/blog/msa2022-hexahedral-mesh-vstetrahedral-comparing-high-quality-meshing.
- [24] özgün, "Ansys Mesh Metrics Explained," Mechead.com, Dec. 15, 2023 https://www.mechead.com/mesh-quality-checking-ansys-workbench/
- [25] "How Hard is Weld?," Practical Machinist Largest Manufacturing Technology Forum on the Web, Jul. 07, 2009. https://www.practicalmachinist.com/forum/threads/how-hard-is-weld.184674/.

Appendix

Arduino Code for Temperature Monitoring using DHT11 Sensor and LCD Display: Code Language

The code is written in C++, specifically for the **Arduino platform**, which utilises a simplified version of C++ that supports microcontroller libraries and hardware interfacing.

Purpose of the Code

This program is designed to:

- Read temperature data from a DHT11 sensor.
- Display the temperature on a **16x2 I2C LCD screen**.
- Activate the **built-in LED** on the Arduino board if the temperature exceeds 45°C.
- Print real-time temperature readings and any errors to the **Serial Monitor**.

Code Overview and Description

// Include required libraries

#include <DHT11.h>

#include <LiquidCrystal I2C.h>

- DHT11.h: Library to interface with the DHT11 sensor.
- LiquidCrystal I2C.h: Library to operate a 16x2 LCD over I2C communication.

LiquidCrystal I2C lcd(0x27, 16, 2);

• Creates an LCD object with I2C address 0x27, 16 columns, and 2 rows.

DHT11 dht11(2);

• Creates a DHT11 object with the sensor connected to digital pin 2 of the Arduino.

Setup Function

void setup() {
Serial.begin(9600);
pinMode(LED_BUILTIN, OUTPUT);

lcd.init(); // initialize LCD
lcd.backlight(); // turn on backlight
lcd.clear(); // clear screen
lcd.setCursor(0, 0);
lcd.print("INDUCTION BASED");
lcd.setCursor(4, 1);
lcd.print("***FSW***");

```
delay(2000);
 lcd.clear();
      Serial.begin(9600);: Starts serial communication at 9600 baud.
      LED BUILTIN (usually pin 13): Configured as output for visual alert (onboard
      LED).
      LCD startup messages: Displays project title ("INDUCTION BASED FSW") for
      2 seconds before clearing the display.
Loop Function
 void loop() {
 int temperature = dht11.readTemperature();
   · Reads temperature data from the DHT11 sensor and stores it in the variable
       temperature.
 if (temperature != DHT11::ERROR_CHECKSUM && temperature !=
 DHT11::ERROR TIMEOUT)
   · Ensures the temperature reading is valid and not corrupted or timed out.
 Serial.print("Temperature: ");
 Serial.print(temperature);
 Serial.println(" °C");
   · Displays temperature reading in the Serial Monitor.
 lcd.setCursor(0, 0);
 lcd.print("Temp: ");
 lcd.print(temperature);
 lcd.print((char)223); // Degree symbol
 lcd.print("C");
   · Displays temperature on the first row of the LCD screen.
 if(temperature < 45){
 digitalWrite(13, LOW); // LED OFF
 } else {
 digitalWrite(13, HIGH); // LED ON
```

• Prints a specific error message if reading fails (like checksum error or timeout).

Turns the built-in LED ON if temperature exceeds 45°C (indicating overheating

condition), else keeps it OFF.

Serial.println(DHT11::getErrorString(temperature));

} else {